A Joint Inversion Method for Breast Imaging using Electromagnetic and Acoustics waves

Ozdemir, Ozgur; Oncu, Ahmet; Van Dongen, Koen W.A.

DOI
10.1109/ICEAA.2018.8520479

Publication date
2018

Document Version
Accepted author manuscript

Published in
Proceedings of the 2018 20th International Conference on Electromagnetics in Advanced Applications, ICEAA 2018

Citation (APA)
Ozdemir, O., Oncu, A., & Van Dongen, K. W. A. (2018). A Joint Inversion Method for Breast Imaging using Electromagnetic and Acoustics waves. In *Proceedings of the 2018 20th International Conference on Electromagnetics in Advanced Applications, ICEAA 2018* (pp. 182-184). Article 8520479 IEEE. https://doi.org/10.1109/ICEAA.2018.8520479

A Joint Inversion Method for Breast Imaging using Electromagnetic and Acoustics waves

Özgür Özdemir
Electronics & Communication Engineering
Istanbul Technical University
Istanbul, Turkey
ozdemiroz3@itu.edu.tr

Koen W.A. van Dongen
Department of Imaging Physics
Delft University of Technology
Delft, the Netherlands
K.W.A.vanDongen@tudelft.nl

Ahmet Öncü
Electrical& Electronics Engineering
Bogazici University
*M*iltek ARGE
Istanbul, Turkey
ahmet.oncu@boun.edu.tr

***Abstract*—Ultrasound and microwave scanners are developed to scan the breast on the presence of cancer. Typically, these modalities are used independently. Here we investigate if we can achieve an improved resolution if we merge both modalities into a single device. In particular, we test if we can improve the resolution of the resulting images by employing a joint inversion method on both data sets as compared to doing two independent inversions leading to two independent images. For the joint inversion an error functional is employed that contains two terms; the first one represents the mismatch between the measured and modeled acoustic and electromagnetic wave fields whereas the second term links the two reconstructed contrast profiles with each other. Results show that joint Born inversion leads indeed to an improved reconstruction as compared to two independent Born inversions.**

***Index Terms*—joint inversion, electromagnetic wave fields, acoustic wave fields, breast cancer**

I. Introduction

Breast cancer is among the leading causes of cancer death for women in the Western world [1]. To reduce mortality rate, national screening programs have been introduced. These screening programs mainly use X-ray mammography to scan a breast on the presence of a tumor. Unfortunately, X-ray mammography has some serious shortcomings; it uses ionizing radiation to probe the interior of the breast, the screening is in general painful, and above all it is less suitable to screen dense breasts typical for young women as the healthy glandular tissue will "overshadow" the tumor in the resulting image. To overcome these shortcomings alternative screening modalities are being developed.

Several initiatives have been employed to build devices that use acoustic wave fields to scan the breast on the presence of cancer [2]–[4]. With these modalities variations in the acoustic medium properties are used to differentiate between the healthy tissues and a cancerous lesion [5]. To obtain these properties, various types of imaging and inversion methods may be employed [6]. Besides acoustic waves also microwaves ares used to scan the breast [7]. With these modalities variations in the dielectric medium properties are used to differentiate between tissues [8], [9].

Up to date, all these modalities work independently; the breast is scanned either using acoustic or electromagnetic wave fields. However, one may expect that an improved resolution may be achieved if the breast is scanned using both modalities simultaneously and where the results from both scans are used in a joint inversion method to improve the resolution of the final images. These type of approaches have already been employed succesfully for geophysical applications [10], but not for medical applications.

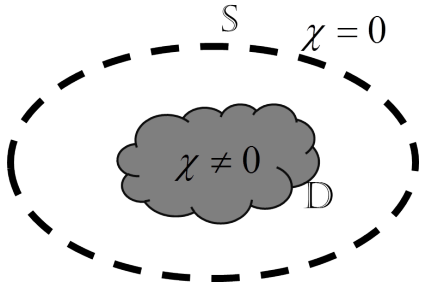

Fig. 1. Schematic representation of the scanning system. The acoustic and electromagnetic sources and receivers are located on a surface $\mathbb{S}$ in the homogeneous background medium. $\mathbb{S}$ encloses the region of interest $\mathbb{D}$ with spatially varying acoustic and dielectric medium properties and with $\mathbb{S} \cap \mathbb{D} = \emptyset$.

To test the feasibility of joint inversion we introduce the underlying theory in section II. In section III we show preliminary results obtained with separate and joined inversion, followed by a conclusion in section IV.

II. Theory

A. Acoustic wave fields

For lossless media with constant volume density of mass ρ_0 and spatially varying speed-of-sound $c(\boldsymbol{x})$, the acoustic pressure wave field $p(\boldsymbol{x}, t)$ at the location $\boldsymbol{x}$ and time instant t is generated by a primary acoustic source $S_A(\boldsymbol{x}, t)$. The resulting wave field governs the scalar wave equation

$$\nabla^2 p(\boldsymbol{x}, t) - \frac{1}{c^2(\boldsymbol{x})} \frac{\partial^2 p(\boldsymbol{x}, t)}{\partial t^2} = -S_A(\boldsymbol{x}, t). \qquad (1)$$

Typically, the sources and the receivers are located on a surface $\mathbb{S}$ in the homogeneous embedding with constant sound speed

c_0. The surface $\mathbb{S}$ encloses the spatial domain of interest $\mathbb{D}$, see Fig. 1.

Equation (1) may be recast into an integral equation of the second kind that reads [11]

$$\hat{p}(\boldsymbol{x}) = \hat{p}^{\mathrm{inc}}(\boldsymbol{x}) + \hat{p}^{\mathrm{sct}}(\boldsymbol{x}), \tag{2}$$

where $\hat{p}^{\mathrm{inc}}(\boldsymbol{x})$ denotes the incident field in the temporal Fourier domain. Here the caret symbol $\hat{}$ is used to denote that a given quantity is defined in the temporal Fourier domain with angular frequency ω. The incident field is obtained by convolving the primary source $\hat{S}(\boldsymbol{x})$ with the Green's function $\hat{G}_A(\boldsymbol{x}-\boldsymbol{x}')$, i.e. the impulse response of the homogeneous embedding, hence

$$\hat{p}^{\mathrm{inc}}(\boldsymbol{x}) = \int\limits_{\boldsymbol{x}'\in\mathbb{S}} \hat{G}_A(\boldsymbol{x}-\boldsymbol{x}')\hat{S}_A(\boldsymbol{x}')\mathrm{d}V(\boldsymbol{x}'). \tag{3}$$

In 2-D, the volume integral in equation (3) reduces to a surface integral and the Green's function $\hat{G}_A(\boldsymbol{x}-\boldsymbol{x}')$ is based on Hankel functions of the first kind, hence

$$\hat{G}_A(\boldsymbol{x}-\boldsymbol{x}') = \frac{-i}{4}H_0^{(1)}(\omega\left|\boldsymbol{x}-\boldsymbol{x}'\right|/c_0). \tag{4}$$

The scattered field is denoted by $\hat{p}^{\mathrm{sct}}(\boldsymbol{x})$ and equals

$$\hat{p}^{\mathrm{sct}}(\boldsymbol{x}) = \frac{\omega^2}{c_0^2}\int_{\boldsymbol{x}'\in\mathbb{D}} \hat{G}_A(\boldsymbol{x}-\boldsymbol{x}')\chi_A(\boldsymbol{x}')\hat{p}(\boldsymbol{x}')\mathrm{d}V(\boldsymbol{x}'), \tag{5}$$

with acoustic contrast function $\chi_A(\boldsymbol{x}')$

$$\chi_A(\boldsymbol{x}') = \frac{c_0^2}{c^2(\boldsymbol{x}')} - 1. \tag{6}$$

Clearly, the acoustic contrast is only non-zero within the domain $\mathbb{D}$.

B. Electromagnetic wave fields

Similar to the acoustic case, the propagation of the electric wave field $\hat{\boldsymbol{E}}(\boldsymbol{x})$ in heterogeneous media may be described using integral equations as well. For the electric field, the resulting integral equation reads

$$\hat{\boldsymbol{E}}(\boldsymbol{x}) = \hat{\boldsymbol{E}}^{\mathrm{inc}}(\boldsymbol{x}) + \hat{\boldsymbol{E}}^{\mathrm{sct}}(\boldsymbol{x}). \tag{7}$$

In equation (7) the incident electric field $\hat{\boldsymbol{E}}^{\mathrm{inc}}(\boldsymbol{x})$ is generated by an electric current $\hat{\boldsymbol{J}}(\boldsymbol{x}')$ and equals

$$\hat{\boldsymbol{E}}^{\mathrm{inc}}(\boldsymbol{x}) = \int\limits_{\boldsymbol{x}'\in\mathbb{S}} \hat{G}_E(\boldsymbol{x}-\boldsymbol{x}')\hat{\boldsymbol{J}}(\boldsymbol{x}')\mathrm{d}V(\boldsymbol{x}'), \tag{8}$$

where $\hat{G}_E$ is the electromagnetic Green's function. The scattered electric field $\hat{\boldsymbol{E}}^{\mathrm{sct}}(\boldsymbol{x})$ in equation (7) is reads

$$\hat{\boldsymbol{E}}^{\mathrm{sct}}(\boldsymbol{x}) = k_0^2\int\limits_{\boldsymbol{x}'\in\mathbb{D}} \hat{G}_E(\boldsymbol{x}-\boldsymbol{x}')\chi_E(\boldsymbol{x}')\hat{\boldsymbol{E}}(\boldsymbol{x}')\mathrm{d}V(\boldsymbol{x}'), \tag{9}$$

with wave number $k_0^2 = \omega^2\epsilon_0\mu_0$ where ϵ_0 is the permittivity of vacuum and μ_0 the permeability of the medium. The electric contrast function $\chi_E(\boldsymbol{x}')$ is defined as

$$\chi_E(\boldsymbol{x}') = \frac{k(\boldsymbol{x}')^2}{k_0^2} - 1. \tag{10}$$

C. Joint inversion with structural similarity approach

Determining the unknown contrast function from the measured scattered field is a non-linear inverse problem that is severely ill-posed. In this work, we explore a linearization of the problem based on the Born approximation. This approximation is valid for targets that are small compared to the wave length of the probing wave field and/or whose contrast functions have a small amplitude. The Born approximation approximates the total field inside the object by the incident field and hence neglects the scattered field. Consequently, the acoustics scattered field reads within this approximation as

$$\hat{p}^{\mathrm{sct}}(\boldsymbol{x}) = \omega^2\int_{\boldsymbol{x}'\in\mathbb{D}} \hat{G}(\boldsymbol{x}-\boldsymbol{x}')\chi_A(\boldsymbol{x}')\hat{p}(\boldsymbol{x}')^{\mathrm{inc}}\mathrm{d}V(\boldsymbol{x}'), \tag{11}$$

and the electric scattered field as

$$\hat{\boldsymbol{E}}^{\mathrm{sct}}(\boldsymbol{x}) = k_0^2\int\limits_{\boldsymbol{x}'\in\mathbb{D}} \hat{G}_E(\boldsymbol{x}-\boldsymbol{x}')\chi_E(\boldsymbol{x}')\hat{\boldsymbol{E}}^{\mathrm{inc}}(\boldsymbol{x}')\mathrm{d}V(\boldsymbol{x}'). \tag{12}$$

The joint inversion is accomplished by defining a cost function as a summation of the data errors for each model as shown in equations (11) and (12) and via the difference between the normalized gradients of the contrast functions. Consequently, the resulting error functional equals

$$F(\chi_A,\chi_E) = \frac{\parallel \hat{p}^{\mathrm{sct}} - \hat{G}_A\chi_A\hat{p}^{\mathrm{inc}}\parallel^2}{\parallel \hat{p}^{\mathrm{inc}}\parallel^2} + \frac{\parallel \hat{E}^{\mathrm{sct}} - \hat{G}_E\chi_E\hat{E}^{\mathrm{inc}}\parallel^2}{\parallel \hat{E}^{\mathrm{inc}}\parallel^2} + \beta\parallel \nabla{\chi_E}^N - \nabla{\chi_A}^N\parallel^2, \tag{13}$$

where β is the regularization parameter, and ${\chi_E}^N$ and ${\chi_A}^N$ are the normalized contrast functions. In order to take advantage of the structural similarity of the acoustics and electromagnetic models, we include in our cost function a regularization term based on the gradients of the two contrast functions. Finally a Conjugate Gradient method is employed for the minimization of the cost function.

III. Numerical Results

In order to verify the proposed method, we consider the reconstruction of the synhetic breast model [12] given in Fig. 2(a) and Fig. 2(b). Here, a circular scanning system enclosing the breast is considered. The system contains 30 acoustic/electromagnetic transmitters and 50 acoustic/electromagnetic receivers equally distributed on the circular array. For the electromagnetic measurements we consider a single frequency of 2 GHz and for the acoustics measurements the two frequencies 60 and 70 kHz. The domain of interest is a squared region of 13 cm by 13 cm that is discretized into 64×64 cells.

We first reconstruct the acoustics and electromagnetic contrasts separately, i.e. $\beta = 0$. The inversion results are given in Fig. 2(c) and Fig. 2(d). It can be seen that the acoustics contrast function is reconstructed quite accurately, however, the electromagnetic contrast function does not provide any detail of the breast. The proposed algorithm is then applied with $\beta = 1$ to improve the electromagnetic reconstruction by

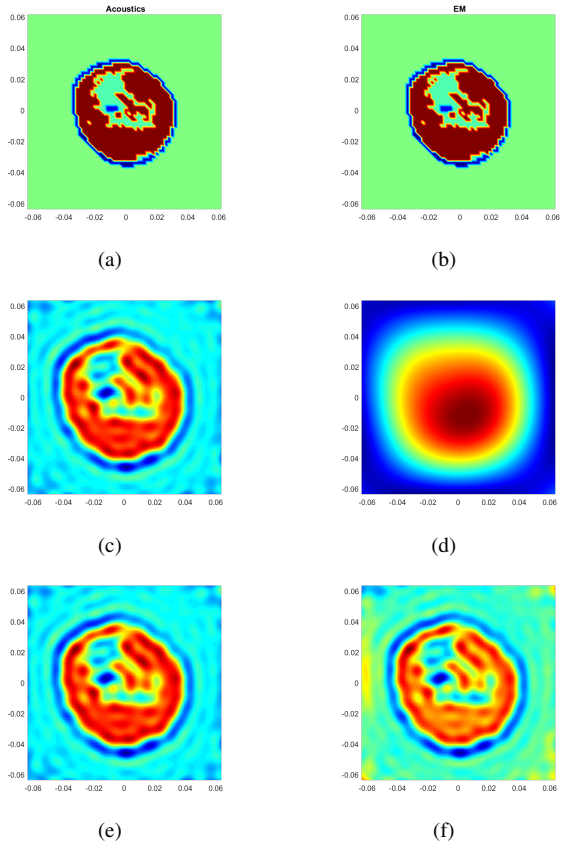

Fig. 2. The synthetic acoustic (a) and electromagnetic (b) models are first reconstructed separately yielding (c) and (d). Next, a joint inversion is applied leading to the reconstructions (e) and (f) with the acoustic model (e) serving as input for the inversion.

taking the acoustic reconstruction into account, see Fig. 2(e) and Fig. 2(f). It is clear that the use of the reconstructed acoustic contrast as an input for the inversion dramatically improves the resolution of the electromagnetic reconstruction.

IV. Conclusion

In this paper, we propose a joint Born inversion algorithm to improve the resolution for ultrasound and electromagnetic imaging for breast cancer detection. The method is tested on a synthetic cancerous breast. We have shown through numerical experiments that the resolution of the reconstructed electromagnetic contrast is improved by using joint inversion.

References

[1] R.L. Siegel, K.D. Miller, and A. Jemal, "Cancer Statistics, 2017," CA Cancer J. Clin. vol. 76(1), pp. 7-30, January 2017.

[2] R. Stotzka, J. Wrfel, T.O. Mller, and H. Gemmeke, "Medical imaging by ultrasound computer tomography," Proc. SPIE Med. Imag., pp. 110-119, 2002.

[3] N.V. Ruiter, T. Hopp, M. Zapf, A. Menshikov, C. Kaiser, and H. Gemmeke, "3D Ultrasound Computer Tomography for Breast Cancer Diagnosis at KIT: an Overview," Proc. International Workshop on Medical Ultrasound Tomography, Speyer Germany, pp. 205-216, November 2017.

[4] L. Heijnsdijk, E. Jansen, U. Taskin, H. den Bok, E. Bergsma, E. Noothout, N. de Jong, and K.W.A. van Dongen, "First steps towards the Delft Breast Ultrasound Scanning System (DBUS)," Proc. International Workshop on Medical Ultrasound Tomography, pp. 131-136, November 2017.

[5] L. Keijzer, M. Lagendijk, N. Stigter, C.H.M. van Deurzen, C. verhoef, W. van Lankeren, L.B. Koppert, and K.W.A. van Dongen, "Measurement of the speed of sound, attenuation and mass density of fresh breast tissue," Proc. International Workshop on Medical Ultrasound Tomography, pp. 369-384, November 2017.

[6] N. Ozmen, R. Dapp, M. Zapf, H. Gemmeke, N.V. Ruiter, and K.W.A. van Dongen, "Comparing different ultrasound imaging methods for breast cancer detection," IEEE Transactions on Ultrasonics, Ferroelectrics, and Frequency Control, vol. 62(4), pp. 637-646, April 2015.

[7] L.L. Wang, "Microwave Sensors for Breast Cancer Detection," Sensors, vol. 18(2), February 2018.

[8] K.R. Foster and H.P. Schwan, "Dielectric properties of tissues and biological materials: A critical review," CRIT Rev. Biomed. Eng., vol. 17(1), pp. 25–104, 1989.

[9] M.S.S. Alwan, and Z. Katbay "Investigation of tumor using an antenna scanning system," Proc. IEEE 2014 Mediterranean Microwave Symp., 2014.

[10] T. Lan, H. Liu, N. Liu, J. Li, F. Han, and Q.H. Liu, "Joint Inversion of Electromagnetic and Seismic Data Based on Structural Constraints Using Variational Born Iteration Method," in IEEE Transactions on Geoscience and Remote Sensing, vol. 56(1), pp. 436-445, January 2018.

[11] A.T. de Hoop, Handbook of Radiation and Scattering of Waves. London, Academic Press, 1995.

[12] J.F. Bakker, M.M. Paulides, I.M. Obdeijn, G.C. van Rhoon, and K.W.A. van Dongen, "An ultrasound cylindrical phased array for deep heating in the breast: theoretical design using heterogeneous models," Physics in Medicine & Biology, vol. 54(10), pp. 3201-3215, 2009.